CC BY

http://dx.doi.org/10.35596/1729-7648-2022-20-1-40-47

Original paper

UDC 621.382.323

LARGE SIGNAL PERFORMANCE OF THE GALLIUM NITRIDE HETEROSTRUCTURE FIELD-EFFECT TRANSISTOR WITH A GRAPHENE HEAT-REMOVAL SYSTEM

VLADISLAV S. VOLCHECK, VIKTOR R. STEMPITSKY

Belarusian State University of Informatics and Radioelectronics (Minsk, Republic of Belarus)

Submitted 16 August 2021

© Belarusian State University of Informatics and Radioelectronics, 2022

Abstract. The self-heating effect exerts a considerable influence on the characteristics of high-power electronic and optoelectronic devices based on gallium nitride. An extremely non-uniform distribution of the dissipated power and a rise in the average temperature in the gallium nitride heterostructure field-effect transistor lead to the formation of a hot spot near the conductive channel and result in the degradation of the drain current, power gain and device reliability. The purpose of this work is to design a gallium nitride heterostructure field-effect transistor with an effective graphene heat-removal system and to study using numerical simulation the thermal phenomena specific to it. The object of the research is the device structure formed on sapphire with a graphene heat-spreading element placed on its top surface and a trench in the passivation layer filled with diamond grown by chemical vapor deposition. The subject of the research is the large signal performance quantities. The simulation results confirm the effectiveness of the heat-removal system integrated into the heterostructure field-effect transistor and leading to the suppression of the self-heating effect and to the improvement of the device performance. The advantage of our concept is that the heat-spreading element is structurally connected with a heat sink and is designed to remove the heat immediately from the maximum temperature area through the trench in which a high thermal conductivity material is deposited. The results of this work can be used by the electronics industry of the Republic of Belarus for developing the hardware components of gallium nitride power electronics.

Keywords: diamond, gallium nitride, graphene, heat-removal system, heterostructure field-effect transistor, large signal performance, power electronics, thermal conductivity.

Conflict of interests. The authors declare no conflict of interests.

Gratitude. This work is supported by the grant 3.1 of Belarusian National Scientific Research Program "Photonics and Electronics for Innovations". The authors would like to express special thanks to Baranova M.S. and Hvazdouski D.C. for providing the data on the thermal conductivity of the (Al,Ga)N material system.

For citation. Volcheck V.S., Stempitsky V.R. Large Signal Performance of the Gallium Nitride Heterostructure Field-Effect Transistor With a Graphene Heat-Removal System. Doklady BGUIR. 2022; 20(1): 40-47.

Introduction

Since its invention forty years ago, the heterostructure field-effect transistor, or high electron mobility transistor (HEMT), has continued to achieve widespread use and drive innovation in the field of information and communications technology. Able to allow for low-noise operation at frequencies up to the millimeter wave band, HEMTs are used in a wide variety of applications, including wireless

Internet and computer networking access systems, cellular phones, navigation systems and satellite broadcast receivers. Furthermore, research and development activities undertaken by corporations and governments in improving and commercializing the novel technology are expanding rapidly all over the world. In addition to standard gallium arsenide HEMTs, the development of ultra-high-frequency indium phosphide and low-power/high-frequency gallium nitride (GaN) transistors is advancing at a lively pace. The deep interest in GaN stems from several factors. First, the wide band gap of 3.4 eV yields a high breakdown voltage, which enables high-power operation. Second, the saturation velocity of electrons in GaN is over a factor of two larger than that in silicon, which is valuable for high-speed operation. Besides, the electrical polarization effects that dominate especially at interfaces result in the induction of a very high electron concentration. Owing to these features, GaN HEMTs can operate at extremely high power densities of tens of watts per millimeter of the gate width. Nevertheless, at such power levels, the dissipated power is non-uniformly distributed and the average temperature is risen, leading to the formation of a hot spot near the conductive channel and resulting in the degradation of the drain current, power gain and device reliability [1]. To minimize the self-heating effect in GaN HEMTs, a variety of thermal solutions has been attempted. These include diamond substrate [2], flip-chip bonding [3], backside metal deposition [4] and heat-spreading element [1]. In spite of all these efforts, the problem of the hot spots still persists.

We have recently investigated [5] the DC and small signal performance of the transistors with a graphene heat-removal system closely resembling that used by Yan et al. [1]. The graphene layers are connected to a heat sink outside the device structure and designed specifically to remove the heat immediately from the maximum temperature region, thus providing an additional heat-escape channel. To enhance the graphene heat-removal system, we have proposed [6] the formation of a trench in the passivation layer in which a high thermal conductivity material, such as boron nitride, boron arsenide or synthetic diamond is deposited. This paper is dedicated to the large signal performance quantities of the GaN HEMT with diamond grown by chemical vapor deposition (CVD) employed as a filler of the trench.

Device structure

The main object of the research is a GaN HEMT formed on sapphire (Al_2O_3) with a graphene heat-spreading element placed on its upper surface and a trench in the passivation layer where CVD-diamond is deposited. It is shown in Fig. 1 and hereinafter referred to as variant C. After the solidus signs, the region thicknesses are indicated.

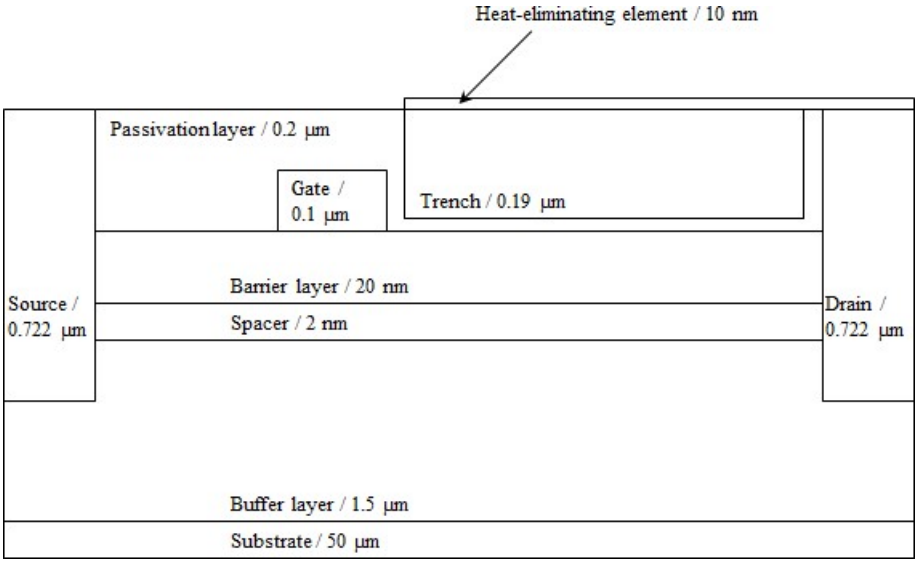

Fig. 1. GaN HEMT with a graphene heat-spreading element and a trench in the passivation layer filled with CVD-diamond

The materials of the buffer, spacer, barrier and passivation layers are GaN, aluminum nitride (AlN), aluminum gallium nitride ($Al_{0.2}Ga_{0.8}N$) and silicon nitride (Si_3N_4), respectively. The distances

source–gate and gate–drain equal to 2 and 5 μm. The gate length is 0.5 μm. The length of the trench located exactly between the gate and the drain equals to 4.8 μm. The graphene heat-spreading element is 5.9 μm long. The width of the transistor is 0.5 mm.

To produce the trench in Si_3N_4, reactive ion etching in chlorine- or fluorine-containing organic or inorganic compounds can be employed, which enables the creation of a trench with sharp and well-controlled features [7]. In theory, the adhesion of CVD-diamond to Si_3N_4 is ensured by a reduction in the interfacial stress due to the similar linear thermal expansion coefficients of these materials [8]. The formation of the graphene heat-spreading element by the highly-oriented pyrolytic graphite exfoliation cannot be accomplished because of the random nature of the process. For this reason, the polymethyl methacrylate-assisted method is proposed [1].

To make a comparative analysis of the DC and large signal transient characteristics, in addition to the GaN HEMT variant C, analogous device structures without any heat-removal system (variant A) and with the graphene heat-spreading element only (variant B) were also simulated.

Equations and models

The device simulation was performed in the framework of the classical drift-diffusion theory of charge transport with the doping density and temperature dependent low- and high-field mobility models of Farahmand et al. [9]. To account for the self-heating effect, a lattice heat flow equation was added to the set of the basic semiconductor device equations. According to the thermodynamically rigorous model of lattice heating [10], the lattice heat flow equation takes the following form:

$$C\frac{\partial T}{\partial t} = \nabla\left(\kappa\nabla T\right) + H, \tag{1}$$

where C is the heat capacity, T is the temperature, κ is the thermal conductivity and H is the heat generation rate.

The heat generation rate takes into account Joule heating, heating and cooling due to carrier generation and recombination, the Peltier and the Thomson effects. As Joule heating is the dominant heat generation process, the other mechanisms were neglected.

Thermal conductivity is known to be a parameter strongly dependent on temperature. This is critical to take into consideration during simulation, as the temperature developed due to self-heating is very sensitive to the thermal conductivities of certain areas of the device. Otherwise, a significant error may occur. The temperature dependence of the thermal conductivity of AlN, GaN, Al_2O_3 [11] and CVD-diamond [12] is expressed as

$$\kappa = \kappa_{300}\left(\frac{T}{300}\right)^{\alpha}, \tag{2}$$

where κ_{300} is the thermal conductivity at 300 K and α is the temperature dependence coefficient.

The thermal conductivity values of the AlN/GaN system were derived using a combination of ab initio simulations and solutions of the linearized phonon Boltzmann transport equation.

The parameters of Eq. (2) are listed in Table 1.

Table 1. Thermal conductivity model parameters

Parameter	Material			
	AlN	GaN	Al_2O_3	CVD-diamond
κ_{300} (W/(cm·K))	3.89	2.58	0.39	21.74
α	–1.28	–1.03	–1.19	–1.17

The thermal conductivity of AlGaN is determined by

$$\kappa\left(Al_xGa_{1-x}N\right) = \left(\frac{x}{\kappa\left(AlN\right)} + \frac{1-x}{\kappa\left(GaN\right)} + \left(3{,}65\cdot10^{-5}T - 2{,}21\cdot10^{-3}\right)x\left(1-x\right)\right)^{-1}, \tag{3}$$

where x is the composition fraction.

The thermal conductivity of amorphous Si_3N_4 equals to 0.021 W/(cm·K) [13].

Simulation results

A series of DC and large signal transient simulations was performed under the following set of conditions:

– the barrier layer is undoped;

– iron-induced deep-level acceptor centers treated as trap states with an energy of 0.7 eV below the conduction band minimum are introduced in the buffer layer, the distribution of the density of states for these acceptor centers corresponds to the profile denoted as “low-Fe” in [14];

– a scale factor of 0.6 is applied to both the spontaneous and piezoelectric polarization terms;

– lumped resistances of 50 Ω are connected to both the gate and drain electrodes;

– the heat transfer coefficients between the substrate and the ambient air as well as between the right side of the heat-spreading element and the ambient air are taken to be infinitely large to make the temperature values at the lower surface of the substrate and at the right edge of the heat-spreading element rigid and equal to 300 K;

– since graphene is not available in the device simulator we use (the parameters of graphene are not stored in the database), the material of the heat-spreading element is treated as a conductor (defined to be a part of the drain electrode) with a thermal conductivity value of 50 W/(cm·K) [15].

The impairment of the DC characteristics of GaN HEMTs attributed to the self-heating effect becomes more pronounced at sufficiently high drain-source voltages (V_{DS}). Fig. 2 presents the drain current vs. gate-source voltage (V_{GS}) and transconductance vs. gate-source voltage characteristics of the GaN HEMT variants A–C and provides a direct comparison with the data obtained by isothermal simulation at 300 K. The drain-source voltage is 15 V.

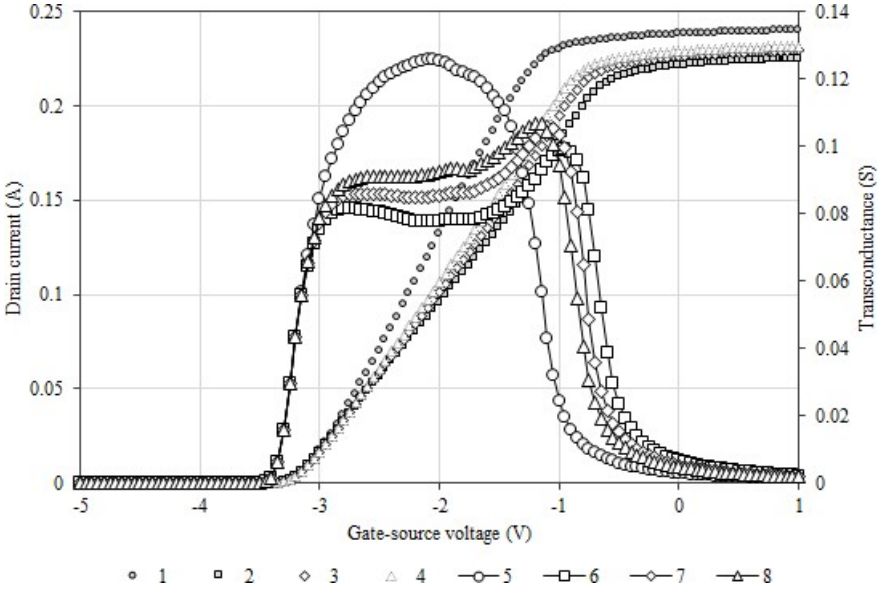

Fig. 2. Input DC characteristics at V_{DS} = 15 V (1 and 5 – no self-heating; 2 and 6 – variant A; 3 and 7 – variant B; 4 and 8 – variant C): 1–4 – drain current; 5–8 – transconductance

At V_{GS} = –2 V, the peak temperature of the GaN HEMT without a heat-removal system rises to 340.7 K, which leads to a reduction in both the drain current by 27.3 %, from 0.132 to 0.096 A, and the transconductance by 37.6 %, from 0.125 to 0.078 S. The placement of the heat-spreading element on top of the transistor results in a 5.2 % increase in the drain current, from 0.096 to 0.101 A, and in a 9.0 % improvement in the transconductance, from 0.078 to 0.085 S. The formation of the trench in the passivation layer filled with CVD-diamond in addition to the graphene layers gives a 10.4 % increase in the drain current, from 0.096 to 0.106 A, and also a 17.9 % improvement in the transconductance, from 0.078 to 0.092 S.

In Fig. 3, the drain current vs. drain-source voltage characteristics are shown. The gate-source voltage is –2 V.

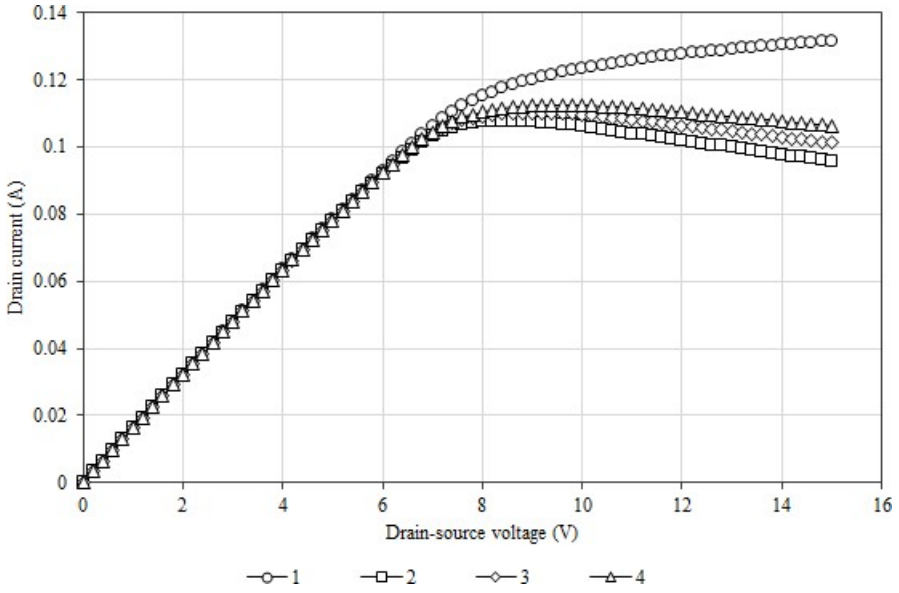

Fig. 3. Drain current vs. drain-source voltage characteristics at V_{GS} = –2 V (1 – no self-heating; 2 – variant A; 3 – variant B; 4 – variant C)

To calculate the large signal performance quantities, the GaN HEMTs were overdriven into heavy distortion at the DC operating point of V_{GS} = –2 V and V_{DS} = 15 V. To this purpose, a sequence of sinusoidal waveforms with amplitudes increasing from 1 to 4 V and frequencies of 2 and 4 GHz was consecutively applied to the gate electrode. Each of these signal levels was simulated for a single period in the time domain. Fig. 4 presents the output power vs. input power (P_{IN}) and power gain vs. input power characteristics determined at 2 GHz.

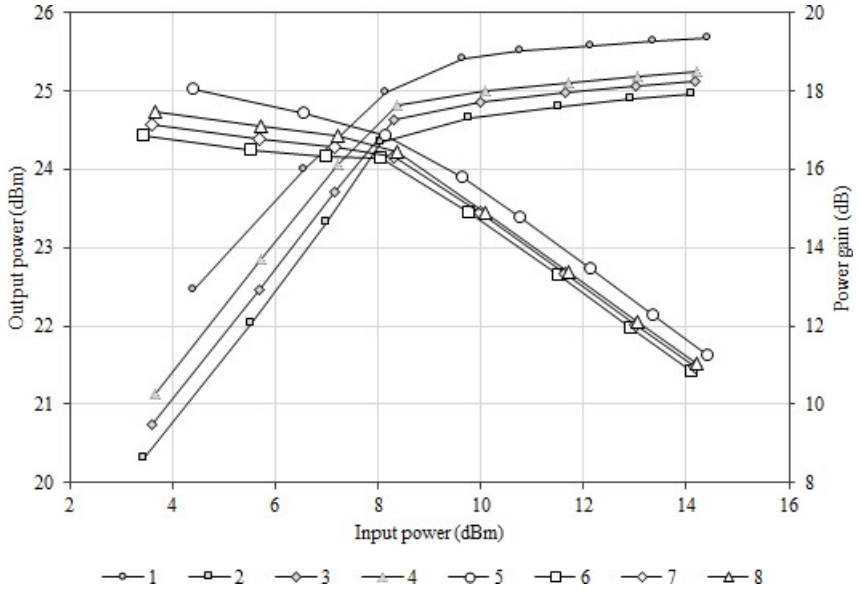

Fig. 4. Large signal performance quantities at 2 GHz (1 and 5 – no self-heating; 2 and 6 –variant A; 3 and 7 – variant B; 4 and 8 – variant C): 1–4 – output power; 5–8 – power gain

The degradation of the DC performance of GaN HEMTs will definitely have an adverse effect on their large signal transient characteristics. Considering the calculations at 2 GHz, at P_{IN} = 14 dBm, the output power is decreased by 2.8 %, from 25.659 to 24.952 dBm, while the power gain is reduced by 6.1 %, from 11.659 to 10.949 dB. The GaN HEMT variant B offers an 0.7 % increase in the output power, from 24.952 to 25.121 dBm, and also a 1.6 % improvement in the power gain, from 10.949 to 11.120 dB. The values for the variant C are 1.1 % (an increase to 25.227 dBm) and 2.6 % (an increase to 11.233 dB), respectively.

The power-added efficiency as a function of the input power determined at 2 GHz is given in Fig. 5.

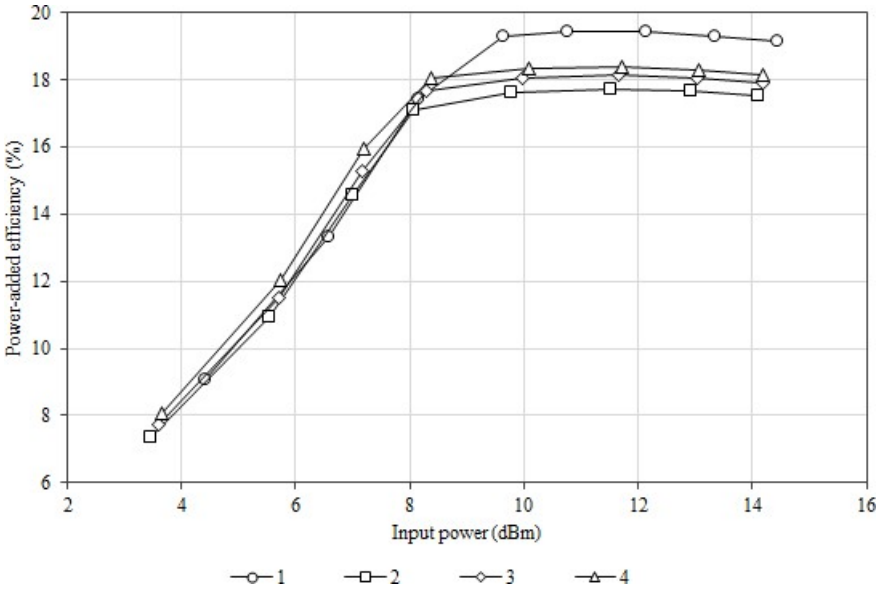

Fig. 5. Power-added efficiency as a function of the input power at 2 GHz (1 – no self-heating; 2 – variant A; 3 – variant B; 4 – variant C)

The maximum power-added efficiency exhibited by the GaN HEMT without a heat-removal system at 2 GHz is 17.7 %, compared with a value of 19.4 % obtained by the isothermal simulation at 300 K. The values of 18.1 % and 18.4 % are achieved for the GaN HEMT variants B and C.

The output power vs. input power and power gain vs. input power characteristics determined at 4 GHz are presented in Fig. 6.

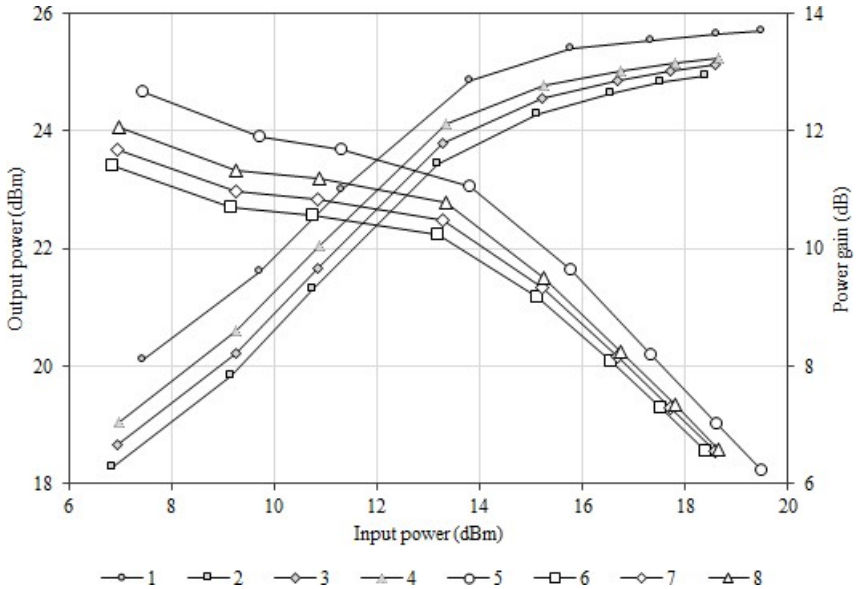

Fig. 6. Large signal performance quantities at 4 GHz (1 and 5 – no self-heating; 2 and 6 –variant A; 3 and 7 – variant B; 4 and 8 – variant C): 1–4 – output power; 5–8 – power gain

In this case, the output power at P_{IN} = 14 dBm is decreased due to the self-heating effect by 4.4 %, from 24.900 to 23.792 dBm, while the power gain drops by 10.2 %, from 10.900 to 9.785 dB. The GaN HEMT variant B offers a 1.2 % increase in the output power, from 23.792 to 24.076 dBm, and also a 3.0 % improvement in the power gain, from 9.785 to 10.076 dB. The values for the variant C are 2.3 % (an increase to 24.337 dBm) and 5.6 % (an increase to 10.337 dB), respectively.

The power-added efficiency as a function of the input power determined at 4 GHz is given in Fig. 7.

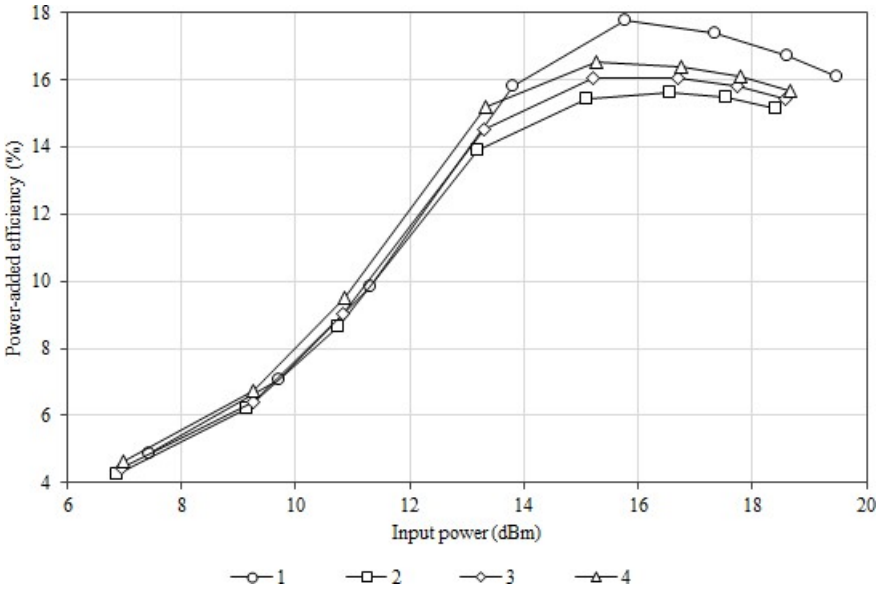

Fig. 7. Power-added efficiency as a function of the input power at 4 GHz (1 – no self-heating; 2 – variant A; 3 – variant B; 4 – variant C)

The maximum power-added efficiency exhibited by the GaN HEMT without a heat-removal system at 4 GHz is 15.6 %, compared with a value of 17.8 % obtained by the isothermal simulation at 300 K. The values of 16.1 % and 16.5 % are achieved for the GaN HEMT variants B and C.

Conclusions

A series of the DC and large signal transient simulations was carried out for GaN HEMTs with graphene heat-spreading elements. One of the two devices featured a trench in the passivation layer filled with CVD-diamond as an enhancement of the heat-escape channel. The simulation results confirm the effectiveness of the trench-based heat-removal system, which leads to the suppression of the self-heating effect and to the improvement of the device performance. When operated at V_{GS} = – 2 V and V_{DS} = 15 V, the maximum power-added efficiency of 18.4 % (16.5 %) was achieved at 2 GHz (4 GHz), compared with 17.7 % (15.6 %) obtained in the absence of a heat-removal system.

References

1. Yan Z., Liu G., Khan J.M., Balandin A.A. Graphene Quilts for Thermal Management of High-Power GaN Transistors. *Nature Communications*. 2012;3:827. DOI: 10.1038/ncomms1828.
2. Hirama K., Taniyasu Y., Kasu M. AlGaN/GaN High-Electron Mobility Transistors with Low Thermal Resistance Grown on Single-Crystal Diamond (111) Substrates by Metalorganic Vapor-Phase Epitaxy. *Applied Physics Letters*. 2011;98(16):162112. DOI: 10.1063/1.3574531.
3. Sun J., Fatima H., Koudymov A., Chitnis A., Hu X., Wang H.-M., Zhang J., Simin G., Yang J., Asif Khan M. Thermal Management of AlGaN-GaN HFETs on Sapphire Using Flip-Chip Bonding with Epoxy Underfill. *IEEE Electron Device Letters*. 2003;24(6):375-377. DOI: 10.1109/LED.2003.813362.
4. Pavlidis G., Kim S.H., Abid I., Zegaoui M., Medjdoub F., Graham S. The Effects of AlN and Copper Back Side Deposition on the Performance of Etched Back GaN/Si HEMTs. *IEEE Electron Device Letters*. 2019;40(7):1060-1063. DOI: 10.1109/LED.2019.2915984.
5. Volcheck V.S., Lovshenko I.Yu., Shandarovich V.T., Dao Dinh Ha. Gallium Nitride High Electron Mobility Transistor with an Effective Graphene-Based Heat Removal System. *Doklady BGUIR*. 2020;18(3):72-80. DOI: 10.35596/1729-7648-2020-18-3-72-80.
6. Volcheck V.S., Stempitsky V.R. Gallium nitride heterostructure field-effect transistor with a heat-removal system based on a trench in the passivation layer filled by a high thermal conductivity material. *Doklady BGUIR* 2021;19(6):74-82. DOI: 10.35596/1729-7648-2021-19-6-74-82.
7. Pant B.D., Tandon U.S. Etching of Silicon Nitride in CCl2F2, CHF3, SiF4, and SF6 Reactive Plasma: A Comparative Study. *Plasma Chemistry and Plasma Processing*. 1999;19(4):545-563. DOI: 10.1023/A:1021886511288.

8. Bland H.A., Thomas E.L.H., Klemencic G.M., Mandal S., Morgan D.J., Papageorgiou A., Jones T.G., Williams O.A. Superconducting Diamond on Silicon Nitride for Device Applications. *Scientific Reports*. 2019;9:2911. DOI: 10.1038/s41598-019-39707-z.
9. Farahmand M., Garetto C., Bellotti E., Brennan K.F., Goano M., Ghillino E., Ghione G., Albrecht J.D., Ruden P.P. Monte Carlo Simulation of Electron Transport in the III-Nitride Wurtzite Phase Materials System: Binaries and Ternaries. *IEEE Transactions on Electron Devices*. 2001;48(3):535-542. DOI: 10.1109/16.906448.
10. Wachutka G.K. Rigorous Thermodynamic Treatment of Heat Generation and Conduction in Semiconductor Device Modeling. *IEEE Transactions on Computer-Aided Design*. 1990;9(11):1141-1149. DOI: 10.1109/43.62751.
11. Dongre B., Carrete J., Mingo N., Madsen G.K.H. Ab Initio Lattice Thermal Conductivity of Bulk and Thin-Film α-Al_2O_3. *MRS Communications*. 2018;8(3):1119-1123. DOI: 10.1557/mrc.2018.161.
12. Feng T., Lindsay L., Ruan X. Four-Phonon Scattering Significantly Reduces Intrinsic Thermal Conductivity of Solids. *Physical Review B*. 2017;96:161201(R). DOI: 10.1103/PhysRevB.96.161201.
13. Stojanovic N., Yun J., Washington E.B.K., Berg J.M., Holtz M.W., Temkin H. Thin-Film Thermal Conductivity Measurement Using Microelectrothermal Test Structures and Finite-Element-Model-Based Data Analysis. *Journal of Microelectromechanical Systems*. 2007;16(5):1269-1275. DOI: 10.1109/JMEMS.2007.900877.
14. Dao Dinh Ha, Trung Tran Tuan, Volcheck V.S., Stempitsky V.R. Iron-Induced Acceptor Centers in the Gallium Nitride High Electron Mobility Transistor: Thermal Simulation and Analysis. *2019 International Conference on Advanced Technologies for Communications (ATC)*. 2019:308-312. вс
15. Balandin A.A. Thermal Properties of Graphene and Nanostructured Carbon Materials. *Nature Materials*. 2011;10:569-581. DOI: 10.1038/NMAT3064.

Authors' contribution

Volcheck V.S. adjusted the physical models used in the simulation, calculated a series of the DC and large signal transient characteristics of the GaN HEMTs, prepared the manuscript.

Stempitsky V.R. researched the self-heating effect and its impact on the performance of high-power GaN HEMTs, formulated the purpose of the work.

Information about the authors

Volcheck V.S., Researcher at the R&D laboratory 4.4 of R&D Department of the Belarusian State University of Informatics and Radioelectronics.

Stempitsky V.R., Cand. of Sci., Associate Professor, Vice Rector for R&D Department of the Belarusian State University of Informatics and Radioelectronics.

Address for correspondence

220013, Republic of Belarus, Minsk, P. Brovki st., 6,
Belarusian State University of Informatics and Radioelectronics;
tel. +375-17-293-84-09;
e-mail: vlad.volchek@bsuir.by
Volcheck Vladislav Sergeevich